

Probing Tensor Monopoles and Gerbe Invariants in Three-Dimensional Topological Matter

Wojciech J. Jankowski,^{1,*} Robert-Jan Slager,^{2,1} and Giandomenico Palumbo^{3,†}

¹*Theory of Condensed Matter Group, Cavendish Laboratory, University of Cambridge, J. J. Thomson Avenue, Cambridge CB3 0HE, UK*

²*Department of Physics and Astronomy, University of Manchester, Oxford Road, Manchester M13 9PL, UK*

³*School of Theoretical Physics, Dublin Institute for Advanced Studies, 10 Burlington Road, Dublin D04 C932, Ireland*

(Dated: July 31, 2025)

We show that momentum-space tensor monopoles corresponding to nontrivial vector bundle generalizations, known as bundle gerbes, can be realized in bands of three-dimensional topological matter with nontrivial Hopf invariants. We provide a universal construction of tensor Berry connections in these topological phases, demonstrating how obstructions therein lead to \mathbb{Z} -quantized bulk magnetoelectric and nonlinear optical phenomena. We then pinpoint that these quantum effects are supported by intraband and interband torsion leading to nontrivial Dixmier-Douady classes in most known Hopf phases and in more general topological insulators realizing gerbe invariants falling beyond the tenfold classification of topological phases of matter. We furthermore provide an *interacting* generalization upon introducing many-body gerbe invariants by employing twisted boundary conditions. This opens an avenue to study gerbe invariants realized through higher-dimensional charge fractionalizations that can be electromagnetically probed.

Introduction.— A key manifestation of topology in physics is embodied by quantization conditions [1]. Fundamentally, physical topological quantizations can be understood in terms of monopole structures. Examples range from the quantization of charge in particle physics in the form of Abelian Dirac monopoles [2] to the quantization of the Hall conductivity in condensed matter physics [3, 4]. Monopoles are generally inherently related to topological invariants in quantum field theory, in which there exist different kinds such as the Yang monopole in five dimensions [5] and the 't Hooft-Polyakov monopole associated to non-Abelian gauge theories [6, 7]. Besides Abelian and non-Abelian vector gauge fields, tensorial gauge fields play a central role in high-energy physics, such as in gravity and string theory with relevant applications in condensed matter physics. In particular, the tensorial character of gauge fields allows for a coupling to extended and inhomogeneous force fields, such as strings [8, 9], which provides for an emergence of exotic physical phenomena inaccessible to point-like objects. For instance, suitable symmetric tensor gauge fields have been shown to describe fractons, which are dual to elasticity supporting topological defects in the form of disclinations or dislocations [10, 11], and higher-spin field theory [12], a lower-dimensional version of which has recently been employed to study the p-atic phases of the fractional quantum Hall effect [13].

In string theory, antisymmetric tensor gauge fields known as Kalb-Ramond fields $B_{\mu\nu}$ [8] allow for an existence of monopoles sourcing a higher-order field strength $\mathcal{H}_{\mu\nu\rho}$, known as tensor monopoles [14, 15], which have been experimentally realized in several synthetic matter systems [16–18]. At the same time, the higher flux $\mathcal{H}_{\mu\nu\rho}$ is also manifested via a kinematic term in the Kalb-Ramond Lagrangian, $\mathcal{L} = -\frac{1}{4}\mathcal{H}_{\mu\nu\rho}\mathcal{H}^{\mu\nu\rho}$, analogously to the Maxwell Lagrangian encompassing electrodynamics [19] and in the equations of

motion associated to the topological BF theories [20–22]. Furthermore, besides its natural relation to Abelian gauge theories, it has also been shown that tensorial flux $\mathcal{H}_{\mu\nu\rho}$ can be directly related to the fully antisymmetric components of the torsion tensor in torsionful gravity [9, 23].

Importantly, the mathematical roots of antisymmetric tensorial gauge theories are encoded in gerbe bundles [24, 25], generalizations of vector bundles that naturally deal with cohomology of higher-forms and differential topology in higher dimensions. Relevance of gerbes acquired a recent interest in topological band theory [26–30], and a particularly intensified focus within tensor network constructions for characterizing interacting topological phases of matter [31–36]. One of the main results of this approach is an identification of novel topological classes and invariants known as Dixmier-Douady classes and numbers, respectively [37, 38]. These Dixmier-Douady numbers are defined as integers in odd dimensions, differently from Chern numbers defined in even dimensions.

The main goal of this work is twofold: (i) we provide a novel construction of tensor Berry connections [26–30], i.e., momentum-space Kalb-Ramond fields, for fermionic condensed matter systems that could support not only stable topological invariants, but also delicate topology [39]. Most interestingly, we show that this also leads to interacting generalizations. In addition, (ii) we identify their observable manifestations provided by tensor monopole quantizations embodied by nontrivial Dixmier-Douady classes in topological gapped phases, such as Hopf insulators [40–45] with underlying quaternionic structures [46], which we show to translate into their linear and nonlinear electromagnetic responses. Importantly, we retrieve these quantizations in delicate topological insulators, i.e., falling beyond the tenfold classification based on K-theory [47–49], and unstable against the hybridizations with additional trivial bands [39], showing that the tensorial gauge structures are intrinsic to homotopy-classified phases of matter, i.e., phases with topological invariants defined only under finite multiband partitionings [50]. As such, we propose distinct ways to probe nontrivial bundle gerbe structures

* wjj25@cam.ac.uk

† giandomenico.palumbo@gmail.com

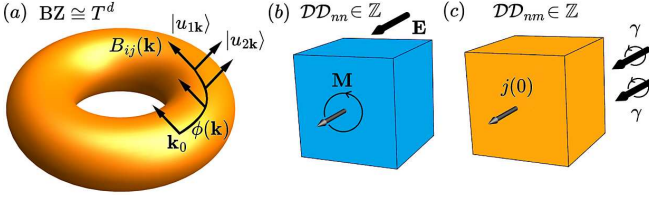


FIG. 1. **Responses from nontrivial gerbe bundles in topological insulators.** (a) Construction of the pseudoscalar $\phi(\mathbf{k})$ and tensor connection $B_{ij}(\mathbf{k})$ from Bloch states $|u_{1\mathbf{k}}\rangle, |u_{2\mathbf{k}}\rangle$ and $\phi(\mathbf{k})$ over d -dimensional Brillouin zone (BZ) realizing topology of a torus (T^d). (b) Magnetoelectric response linear in electric field \mathbf{E} , probing intra-band $\mathcal{DD}_{nm} \in \mathbb{Z}$ invariants. (c) Nonlinear shift current $j(0)$ response to a pair of circularly polarized photons γ , quadratic in electric field, probing interband $\mathcal{DD}_{nm} \in \mathbb{Z}$ ($n \neq m$) gerbe invariants.

and tensorial monopoles in topological phases with nontrivial Dixmier-Douady classes, such as Hopf insulators that realize delicate topology [39].

Gerbe Bundle Invariants.— We now detail the construction of tensorial Berry connections amounting to gerbe bundle invariants, which we further retrieve as observable in certain topological insulators beyond the tenfold classification [47]. We begin with standard vector Berry connections central to Hall phenomena. In condensed matter physics, the Hall phenomena in two dimensions are induced by the Berry curvature flux in the space of momenta [3, 51],

$$F_{xy}^n = \partial_x A_y^n - \partial_y A_x^n, \quad (1)$$

where $A_i^n = i \langle u_{n\mathbf{k}} | \partial_i u_{n\mathbf{k}} \rangle$ is the vectorial Berry connection, \mathbf{k} is a single-particle momentum, $|u_{n\mathbf{k}}\rangle$ is the n -th Bloch band eigenvector, and we use $\partial_i \equiv \partial_{k_i}$ for brevity. Formally, A_i^n is a connection one-form over a line bundle of eigenvectors $|u_{n\mathbf{k}}\rangle$ over Brillouin zone (BZ) in k -space, and can be seen as the momentum-space analog of the electromagnetic potential. In a similar way, an existence of a momentum-space version of the Kalb-Ramond field, dubbed tensor Berry connection B_{ij} , with $i, j = x, y, z$, has been proposed [26–30], which generates the following fluxes of the momentum-space tensorial gauge fields in three dimensions

$$\mathcal{H}_{xyz} = \partial_x B_{yz} + \partial_y B_{zx} + \partial_z B_{xy}. \quad (2)$$

More formally, B_{ij} can be thought of as a connection of the bundle gerbe (see End Matter, App. A, for details), which we here retrieve on gauging fluxes F_{ij} with pseudoscalar fields ϕ [27]. As a central result, we will construct the tensor connection B_{ij} from the Wilson lines of Bloch states.

Crucially, the monopoles in tensor Berry connection fields defined over bundle gerbes provide for nontrivial Dixmier-Douady (\mathcal{DD}) invariants, as an obstruction to Gauss-Ostrogradsky divergence theorem,

$$\mathcal{DD}_{nm} = -\frac{1}{4\pi^2} \int_{\text{BZ}} d^3\mathbf{k} \mathcal{H}_{xyz}^{nm}, \quad (3)$$

with n, m the band indices, which is a higher-dimensional analog of the Chern class quantization as an obstruction to

Stokes's theorem,

$$C_n = \frac{1}{2\pi} \int_{\text{BZ}} d^2\mathbf{k} F_{xy}^n. \quad (4)$$

It is well-known that the Chern class underlies the quantization of the Hall conductivity $\sigma_{xy} = \frac{e^2}{h} \sum_n C_n$ supported by individual occupied bands n [3]. On the contrary, here, we construct \mathcal{H}_{xyz}^{nm} from B_{ij}^{nm} , following Eq. (2), with $B_{ij}^{nm} \equiv \phi_{nm} \mathcal{F}_{ij}^{nm}$, where $\mathcal{F}_{ij}^{nm} = \partial_i A_j^{nm} - \partial_j A_i^{nm}$, with $A_i^{nm} = \langle u_{n\mathbf{k}} | \partial_i u_{m\mathbf{k}} \rangle$ the derivative part of the non-Abelian Berry curvature flux. As such, by construction, $\partial_k \mathcal{F}_{ij}^{nm} + \partial_i \mathcal{F}_{jk}^{nm} + \partial_j \mathcal{F}_{ki}^{nm} = 0$, which shows that tensor monopoles require singular features in $\phi_{nm}(\mathbf{k})$. However, differently from the previous gerbe constructions [26–30, 52], and centrally to this work, here we define the pseudoscalar fields as follows,

$$\phi_{nm}(\mathbf{k}) \equiv \int_{\mathbf{k}_0}^{\mathbf{k}} dk^i A_i^{nm}(\mathbf{k}'), \quad (5)$$

which formally is equivalent to a Wilson line from point $\mathbf{k}_0 = \mathbf{0}$ over the momentum space [see Fig. 1(a)]. In the above, we assumed Einstein summation convention, and by default we choose the shortest path, i.e., geodesic, over parameter space as an integration contour, see Fig. 1(a). We demand that the pseudoscalar fields are real by construction, which for $n \neq m$ must be enforced with an additional symmetry, e.g., spacetime inversion symmetry (\mathcal{PT}), such that the Hamiltonian and the eigenvectors can be written in real gauge [50, 53]. We note that the above construction resembles the dimensional reduction of one-form gauge fields that allows to obtain axion fields in quantum field theory [54, 55]. In fact, such pseudoscalar fields can be seen as momentum-space versions of real-space axions. Notably, shifting the origin $\mathbf{k}_0 = \mathbf{0}$ to another base point \mathbf{k}'_0 , transforms the pseudoscalars as $\phi_{nm}(\mathbf{k}) \rightarrow \phi_{nm}(\mathbf{k}) + \phi_{nm}^0$, with $\phi_{nm}^0 \equiv \int_{\mathbf{k}_0}^{\mathbf{k}'_0} dk^i A_i^{nm}(\mathbf{k}')$. These can be viewed as gauge transformations of the gerbe two-form connections,

$$B_{ij}^{nm} \rightarrow B_{ij}^{nm} + \partial_i \xi_j^{nm} - \partial_j \xi_i^{nm} \equiv B_{ij}^{nm} + \Lambda_{ij}^{nm}, \quad (6)$$

with gauge vectors $\xi_i^{nm} = \phi_{nm}^0 A_i^{nm}$, defining an exact two-form Λ_{ij}^{nm} , which is divergenceless and cannot contribute to the flux \mathcal{H}_{ijk}^{nm} , nor to the \mathcal{DD} invariants. Moreover, specifically for $\phi_{nn} \equiv \int_{\mathbf{k}_0}^{\mathbf{k}} dk^i A_i^n(\mathbf{k}')$, we admit a local transformation $A_i^n(\mathbf{k}) \rightarrow A_i^n(\mathbf{k}) + \partial_i \alpha^n(\mathbf{k})$ on transforming the Bloch states $|u_{n\mathbf{k}}\rangle \rightarrow e^{i\alpha^n(\mathbf{k})} |u_{n\mathbf{k}}\rangle$, $\phi_{nn}(\mathbf{k}) \rightarrow \phi_{nn}(\mathbf{k}) + \alpha^n(\mathbf{k})$. Under the non-Abelian transformations with matrices U , $|u_{m\mathbf{k}}\rangle \rightarrow [U]_{mn} |u_{n\mathbf{k}}\rangle$, the pseudoscalar matrix, $[\Phi]_{nm} \equiv \phi_{nm}$, transforms as $\Phi \rightarrow U\Phi U^\dagger$, consistently with the vector of non-Abelian Berry connection matrices, $[\mathbf{A}]_{nm} \equiv (A_x^{nm}, A_y^{nm}, A_z^{nm})$, $\mathbf{A} \rightarrow U\mathbf{A}U^\dagger$ [30]. By construction, we have $A_i^{nm}(\mathbf{k}) = \partial_i \phi_{nm}(\mathbf{k})$, and hence $\mathcal{H}_{xyz}^{nn} = \epsilon_{abc} A_a^n \partial_b A_c^n$, or $\mathcal{H}_{xyz}^{nn} = \epsilon_{abc} A_a^{nn} \partial_b A_c^{nn}$, which are equal to Abelian Chern-Simons forms amounting to quantized Hopf and real Hopf indices [40, 44–46] in topological insulators, when integrated over single-particle eigenstates across BZ.

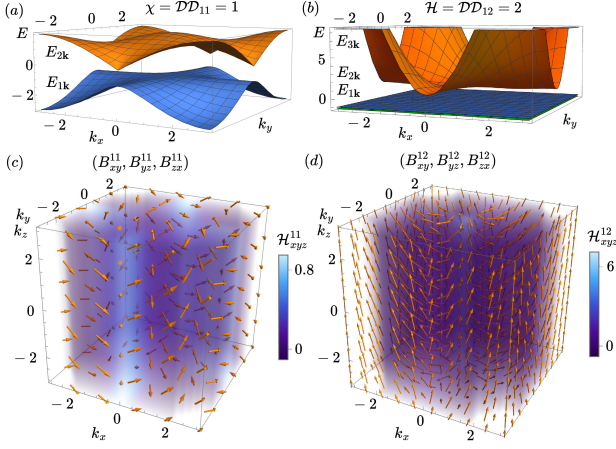


FIG. 2. **Tensor monopoles in topological insulators with Hopf indices.** (a) Band structure of two-band Hopf insulator realizing intra-band $\mathcal{DD}_{11} \in \mathbb{Z}$ invariant at $M = 1$ and (b) three-band real Hopf insulator realizing interband $\mathcal{DD}_{12} \in \mathbb{Z}$ invariant at $M = 3/2$. The bands are shown at momentum $k_z = 0$. (c) Tensor monopole of momentum-space Kalb-Ramond field B_{ij}^{11} yielding flux \mathcal{H}_{ij}^{11} in Hopf insulator with $\chi = 1$. (d) Tensor monopole of Kalb-Ramond field B_{ij}^{12} introducing an interband torsional flux \mathcal{H}_{ij}^{12} in real Hopf-Euler insulator with topological index $\mathcal{H} = 2$.

In the following, we show that the \mathcal{DD} invariants, including intraband gerbe invariants \mathcal{DD}_{nn} , quantize geometric contributions to magnetoelectric responses, providing for \mathbb{Z} quantizations in realistic three-dimensional topological crystallites [see Fig. 1(b)]. Furthermore, we show that the more general interband \mathcal{DD} gerbe invariants \mathcal{DD}_{nm} quantize nonlinear second-order integrated shift responses to circularly polarized light [see Fig. 1(c)].

Gerbes and Magnetoelectric Effects.— Here, we retrieve the gerbe quantization by the \mathcal{DD} invariants in magnetoelectric responses [56–60]. The magnetoelectric tensor α_{ij} yielding orbital magnetization currents (M_i) from electric fields E_j , $M_i = \alpha_{ij}E_j$, consists of topological and nontopological terms (see End Matter, App. B), where the topological term dominates in tenfold-classified topological materials [58]. We find that the trace of topological magnetoelectric coupling amounts to the higher Berry curvature and \mathcal{DD} invariants,

$$\text{Tr } \alpha_{ij}^{\text{top}} = \frac{e^2}{8\pi^2 hc} \int_{\text{BZ}} d^3\mathbf{k} \sum_{n,n'} \mathcal{H}_{xyz}^{nn'} = \frac{e^2}{2hc} \sum_{n,n'} \mathcal{DD}_{nn'}. \quad (7)$$

Here, the Kalb-Ramond flux over occupied bands, $\mathcal{H}_{xyz}^{nn'} = \epsilon_{ijk} T_{ijk}^{nn'}$, admits *intraband* torsion, when $n = n'$, which we introduce as a generalization of the interband torsion [45, 61] (see End Matter, App. C). In particular, in a Hopf insulator [40],

$$\text{Tr } \alpha_{ij}^{\text{top}} = \frac{e^2}{2hc} \mathcal{DD}_{11} = \frac{e^2}{2hc} \chi, \quad (8)$$

with $\chi \in \mathbb{Z}$ the Hopf invariant, consistently with the \mathbb{Z} -quantized Chern-Simons form, $\theta_{\text{CS}} = \pi\chi$ [62], which yields

a \mathbb{Z} -magnetoelectric effect in Hopf insulator, analogously to the \mathbb{Z} -magnetoelectric effect in the chiral three-dimensional insulators retrieved from the winding numbers in the chiral symmetry class AIII [60, 63]. In fact, in these strong topological insulators, the \mathbb{Z} -quantization of the magnetoelectric effect can be also formally explained by employing the gerbe formalism as the three-dimensional winding number coincides with the \mathcal{DD} invariant [27].

In two-band Hopf insulator realizations [40, 41], with an occupied topological band $n = 1$, the invariant reads $\chi = -\frac{1}{4\pi^2} \int_{\text{BZ}} d^3\mathbf{k} [\mathbf{A}_{11} \cdot (\nabla_{\mathbf{k}} \times \mathbf{A}_{11})] \in \mathbb{Z}$, which represents the nontrivial homotopy elements $\pi_3[S^2] \cong \mathbb{Z}$, mathematically corresponding to distinct Hopf fibrations: $S^3 \rightarrow S^2$ [40]. We show the corresponding Hopf bands in Fig. 2(a), tensor monopole [Fig. 2(c)], and topological magnetoelectric response quantized by the gerbe invariant against the corrections from nontopological responses, as a function of topological mass parameter M in Fig. 3(a). For further details on the models, topological classifications, and underlying gerbe structures, see the Supplemental Material (SM) [64].

Moreover, we find that the topological magnetoelectric response is quantized by *interband* \mathcal{DD} invariant in three-band Hopf-Euler insulators with an occupied pair of topological bands $\{|u_{1\mathbf{k}}\rangle, |u_{2\mathbf{k}}\rangle\}$,

$$\text{Tr } \alpha_{ij}^{\text{top}} = \frac{e^2}{2hc} \mathcal{DD}_{12} = \frac{e^2}{2hc} \mathcal{H}, \quad (9)$$

where we define $\mathcal{H} = -\frac{1}{4\pi^2} \int_{\text{BZ}} d^3\mathbf{k} [\mathbf{A}_{12} \cdot \mathbf{E}u_{12}] \in \mathbb{Z}$ which is quantized under \mathcal{PT} spacetime inversion symmetry [45], with $\mathbf{E}u_{12} \equiv \nabla_{\mathbf{k}} \times \mathbf{A}_{12}$ the Euler curvature [65–67]. Under the quantizing symmetry, $\mathcal{H} \in \mathbb{Z}$ furthermore represents distinct nontrivial homotopy elements $\pi_3[S^2] \cong \mathbb{Z}$ [45]. We stress that this quantized magnetoelectric response, which we here show to arise from the gerbe invariant, was not identified in Ref. [45] that introduced the three-band Hopf-Euler band topologies, where a trivial θ angle, $\theta_{\text{CS}} = 0 \pmod{2\pi}$, was only recognized. We show the corresponding Hopf-Euler bands in Fig. 2(b), tensor monopole [Fig. 2(d)], and the magnetoelectric response against the topological mass M for phases with distinct topological index \mathcal{DD}_{12} [Fig. 3(a)], see SM (Sec. I) [64] for details on the models. The identification of the Hopf insulator as a condensed matter realization of a momentum space tensor monopole,

$$\chi = -\frac{1}{4\pi^2} \int_{\text{BZ}} d^3\mathbf{k} \mathcal{H}_{xyz} \in \mathbb{Z}, \quad (10)$$

integer character of which can be magnetoelectrically probed, e.g., within the previously proposed experimental setup [60], is a central result of this work. Furthermore, the N -band generalization of a Hopf insulator [68], is also a tensor monopole, by an analogous reformulation of the invariant as a tensor flux, which we explicitly demonstrate in the SM [64].

Gerbes in Quantized Shift Responses.— In the following, we show how the gerbe structure associated with interband \mathcal{DD}_{nm} invariants ($n \neq m$) can be probed with nonlinear

second order optical responses. Inspired by high energy physics results in real spacetime [23], we here employ the momentum-space correspondence between the gerbe flux and the totally antisymmetric part of the torsion, namely $\mathcal{H}_{ijk}^{mn} = \mathcal{T}_{[ijk]}^{mn}$, with $\mathcal{T}_{[ijk]}^{mn}$ interband torsion, which captures virtual transitions between bands n, m through additional bands p [69–71]. We first recast the torsional sum rule of Ref. [71] for circular shift photoconductivities $\sigma_{ijk}^{\text{shift,C}}(\omega)$ [69] that determine geometric dc photovoltaic current density responses $j_i(0) = \sigma_{ijk}^{\text{shift,C}}(\omega) E_j(\omega) E_k(-\omega)$ from electronic positional shifts [71–76] induced by optical electric fields $E_j(\omega)$, which we further detail and comment in the End Matter (App. C),

$$\begin{aligned} F_{\text{sym}} &\equiv \int_0^{\omega_{\text{max}}} d\omega [\sigma_{xyz}^{\text{shift,C}}(\omega) + \sigma_{yzx}^{\text{shift,C}}(\omega) + \sigma_{zxy}^{\text{shift,C}}(\omega)] \\ &= -\frac{e^3}{4\pi^2 \hbar^2} \int_{\text{BZ}} d^3 \mathbf{k} \sum_{n,n} f_{nm} \mathcal{H}_{xyz}^{mn}. \end{aligned} \quad (11)$$

ω_{max} is an energy cutoff targeting optical transitions between all single-particle states in occupied/unoccupied bands n/m . The filling factor differences $f_{nm} \equiv f_n - f_m$ are fixed on setting a zero-temperature limit, with $f_n = 1$ for occupied and $f_m = 0$ for unoccupied bands, which results in a general torsional quantization from fully occupied bands

$$F_{\text{sym}} = \frac{e^3}{\hbar^2} \sum_{n,m} \mathcal{DD}_{nm}. \quad (12)$$

We show the integrated shift response against the cutoff frequency ω_{max} for phases with distinct topological index \mathcal{DD}_{12} in Fig. 3(b), see SM (Sec. I) [64] for details on the models. While a similar physical quantization condition was retrieved in \mathcal{PT} -symmetric three-band and four-band models [45, 71], the more general gerbe structures providing the quantization as tensor monopoles related to momentum-space tensor Berry connections, as well as their additive character underpinned by Eq. (12), have not been uncovered before. This moreover provides a generalization to arbitrary N -band topologies realizing \mathcal{DD} invariants, beyond the previous four-band and three-band realizations of topological insulators with Hopf indices [44, 45, 71, 77], as the sum over n, m with n occupied and m unoccupied bands is otherwise unconstrained.

Interacting Generalization.— Importantly, the discussed linear and nonlinear electromagnetic responses can also be utilized to study interacting systems. For example, optical probes, such as circular dichroism, have been employed to study interacting two-dimensional topological systems, such as fractional Chern insulators [78]. Generalizing our results to interactions in three-dimensional topological systems central to this work, necessarily involves many-body \mathcal{DD} invariants. Hence, as an outlook, we briefly detail how the \mathcal{DD} invariants can be generalized to interacting systems with twisted boundary conditions analogous to the construction of many-body Chern invariants [3]. We impose twisted boundary on a many-body wavefunction $|\psi(\theta)\rangle$ with twist angles

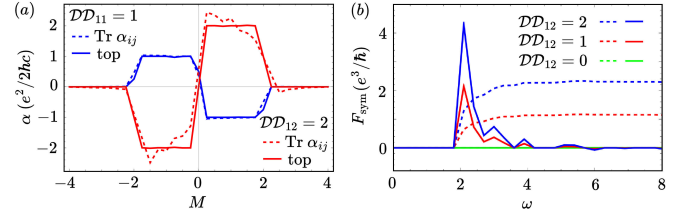


FIG. 3. **Quantized responses and gerbe invariants.** (a) Topological (top) magnetoelectric susceptibility $\text{Tr } \alpha_{ij}^{\text{top}}$ (bold) and total ($\text{Tr } \alpha_{ij}$) magnetoelectric susceptibility (dashed) in Hopf and real Hopf insulators, as a function of topological mass parameter M . Topological phases with $\mathcal{DD}_{11} = 1$, $\mathcal{DD}_{12} = 2$ correspond to $|M| < 2$. The non-topological magnetoelectric response is dominated by the topological contribution. (b) Integrated shift response against cutoff frequency $\omega = \omega_{\text{max}}$ (dashed) for different interband gerbe invariants \mathcal{DD}_{nm} in three-band real Hopf insulators with lower two bands occupied. The frequency resolution (bold) of the integrated response indicates dominant contributions from the Kalb-Ramond flux \mathcal{H}_{xyz}^{nm} due to fermions photoexcited at frequencies directly above the band gap.

$\theta = (\theta_x, \theta_y, \theta_z)$ acting as twisted boundary conditions across linear system size lengths L_i [51], $\psi(\{x_i + L_i\}) = e^{i\theta_i} \psi(\{x_i\})$, where $\{x_i\}$ are coordinates of the single particles constituting the many-body wavefunction in many-body particle coordinate representation, $\psi(\{x_i\}) = \langle \{x_i\} | \psi(\theta) \rangle$. We define the many-body connection, $A_i(\theta) \equiv i \langle \psi(\theta) | \partial_{\theta_i} \psi(\theta) \rangle$, and many-body flux, $F_{ij}(\theta) = \partial_{\theta_i} A_j(\theta) - \partial_{\theta_j} A_i(\theta)$, alongside a pseudoscalar,

$$\phi(\theta) \equiv \int_0^\theta d\theta'_i A_i(\theta'). \quad (13)$$

The combination of flux and pseudoscalar defines a tensor connection $B_{ij}(\theta) = \phi(\theta) F_{ij}(\theta)$. Analogously to the single-particle case, the many-body tensor connection $B_{ij}(\theta)$ transforms as $B_{ij}(\theta) \rightarrow B_{ij}(\theta) + \Lambda_{ij}(\theta)$, with divergenceless two-form $\Lambda_{ij}(\theta)$, under the shift of the initial integration limit specifying the zero of twisted boundary conditions ($\theta = 0$) within the many-body pseudoscalar definition. The many-body tensor connection determines the tensorial flux,

$$\mathcal{H}_{xyz}(\theta) = \partial_{\theta_x} B_{yz}(\theta) + \partial_{\theta_y} B_{zx}(\theta) + \partial_{\theta_z} B_{xy}(\theta), \quad (14)$$

and integrates to a many-body \mathcal{DD}_{MB} invariant,

$$\mathcal{DD}_{\text{MB}} \equiv -\frac{1}{4\pi^2} \iiint d\theta_x d\theta_y d\theta_z \mathcal{H}_{xyz}(\theta) \in \mathbb{Z}. \quad (15)$$

On one hand, in the presence of short-range interactions, and no ground-state degeneracy, we expect that this invariant remains quantized, similarly to the quantization of the first Chern number in two-dimensional interacting systems [79, 80]. On the other hand, in the case of a q -degenerate ($q \in \mathbb{N}$) ground state, we expect the \mathcal{DD}_{MB} invariant to be fractionalizable ($\mathcal{DD}_{\text{MB}} = 1/q$), analogously to the many-body Chern invariant [51, 79]. The fractionalization could possibly be probed with the discussed linear and nonlinear electromagnetic effects that target the gerbe invariants. The realizations

and detailed calculations of fractional \mathcal{DD}_{MB} invariant in specific three-dimensional interacting and topologically ordered phases will be addressed in future work.

Discussion and Conclusion.— We demonstrate that gerbe bundle invariants provided by tensor gauge fields associated with tensor monopoles can be probed in three-dimensional fermionic phases of matter such as Hopf insulators and other topological phases with nontrivial \mathcal{DD} invariants. We retrieve probes of these structures in integer magnetoelectric responses targetting the intraband gerbe invariants, as well as nonlinear optical responses probing interband torsion and gauge-invariant Kalb-Ramond fluxes \mathcal{H}_{ijk}^{nm} selectively at the momentum space sections where the transitions at the photon frequency ω occur, see Fig. 3. In doing so, we provide a unique construction of tensor Berry connections in topological insulators, beyond the conventional Berry connections, showing that momentum-space Kalb-Ramond fields can also be manifestly realized by free fermionic topological phases. As in the case of interactions fractionalizing Chern invariants, we derive the many-body generalization and predict the fractionalization of \mathcal{DD} invariant, here defined under twisted boundary conditions, to arise from many-body ground-state degeneracies. The provided electromagnetic probes could allow to pinpoint a possible existence of fractional topological insulators characterized by the many-body \mathcal{DD} invariant via magnetoelectric and optical phenomena originally retrieved here for integer quantizations under the noninteracting setups.

ACKNOWLEDGMENTS

We thank Aris Alexandradinata, Zory Davoyan, Duncan Haldane, and Hans Hansson for helpful discussions. W.J.J. acknowledges funding from the Rod Smallwood Studentship at Trinity College, Cambridge. R.-J.S. acknowledges funding from a New Investigator Award, EPSRC Grant No. EP/W00187X/1, a EPSRC ERC underwrite Grant No. EP/X025829/1, and a Royal Society exchange Grant No. IES/R1/221060, as well as Trinity College, Cambridge.

[1] Charles Nash and Siddhartha Sen, *Topology and geometry for physicists* (Elsevier, 1988).
 [2] John Preskill, “Magnetic monopoles,” *Annual Review of Nuclear and Particle Science* **34**, 461–530 (1984).
 [3] D. J. Thouless, M. Kohmoto, M. P. Nightingale, and M. den Nijs, “Quantized Hall conductance in a two-dimensional periodic potential,” *Phys. Rev. Lett.* **49**, 405–408 (1982).
 [4] F. D. M. Haldane, “Model for a quantum Hall effect without Landau levels: Condensed-matter realization of the “parity anomaly,”” *Phys. Rev. Lett.* **61**, 2015–2018 (1988).
 [5] Chen Ning Yang, “Generalization of Dirac’s monopole to SU(2) gauge fields,” *J. Math. Phys.(NY);(United States)* **19** (1978).
 [6] Gerardus t Hooft, “Magnetic monopoles in unified theories,” *Nucl. Phys. B* **79**, 276–284 (1974).

[7] Alexander M Polyakov, “Particle spectrum in quantum field theory,” *JETP lett* **20**, 300 (1974).
 [8] Michael Kalb and P. Ramond, “Classical direct interstring action,” *Phys. Rev. D* **9**, 2273–2284 (1974).
 [9] David Tong, “Lectures on String Theory,” (2012), [arXiv:0908.0333 \[hep-th\]](https://arxiv.org/abs/0908.0333).
 [10] Michael Pretko and Leo Radzihovsky, “Fracton-elasticity duality,” *Phys. Rev. Lett.* **120**, 195301 (2018).
 [11] Aron J. Beekman, Jaakko Nissinen, Kai Wu, Ke Liu, Robert-Jan Slager, Zohar Nussinov, Vladimir Cvetkovic, and Jan Zaanen, “Dual gauge field theory of quantum liquid crystals in two dimensions,” *Phys. Rep.* **683**, 1 – 110 (2017), dual gauge field theory of quantum liquid crystals in two dimensions.
 [12] Christian Fronsdal, “Massless fields with integer spin,” *Phys. Rev. D* **18**, 3624–3629 (1978).
 [13] E. Bergshoeff, A. Campoleoni, G. Palumbo, and P. Salgado-Rebolledo, “Massive higher-spin fields in the fractional quantum Hall effect,” *Phys. Rev. B* **110**, 235152 (2024).
 [14] Rafael I Nepomechie, “Magnetic monopoles from antisymmetric tensor gauge fields,” *Physical Review D* **31**, 1921 (1985).
 [15] Peter Orland, “Instantons and disorder in antisymmetric tensor gauge fields,” *Nuclear Physics B* **205**, 107–118 (1982).
 [16] Xinsheng Tan, Dan-Wei Zhang, Wen Zheng, Xiaopei Yang, Shuqing Song, Zhikun Han, Yuqian Dong, Zhimin Wang, Dong Lan, Hui Yan, Shi-Liang Zhu, and Yang Yu, “Experimental observation of tensor monopoles with a superconducting qudit,” *Phys. Rev. Lett.* **126**, 017702 (2021).
 [17] Mo Chen, Changhao Li, Giandomenico Palumbo, Yan-Qing Zhu, Nathan Goldman, and Paola Cappellaro, “A synthetic monopole source of Kalb-Ramond field in diamond,” *Science* **375**, 1017–1020 (2022).
 [18] Qingyang Mo, Shanjun Liang, Cuicui Lu, Jie Zhu, and Shuang Zhang, “Tensor-monopole-induced topological boundary effects in four-dimensional acoustic metamaterials,” *Phys. Rev. Lett.* **134**, 186601 (2025).
 [19] Marc Henneaux and Claudio Teitelboim, “p-form electrodynamics,” *Foundations of Physics* **16**, 593–617 (1986).
 [20] Alberto S. Cattaneo, Paolo Cotta-Ramusino, Jürg Fröhlich, and Maurizio Martellini, “Topological BF theories in 3 and 4 dimensions,” *Journal of Mathematical Physics* **36**, 6137–6160 (1995).
 [21] TH Hansson, Vadim Oganesyan, and Shivaji Lal Sondhi, “Superconductors are topologically ordered,” *Annals of Physics* **313**, 497–538 (2004).
 [22] Giandomenico Palumbo, “Topological phases for extended objects: Semiclassical phase-space approach with tensorial coordinates,” *Phys. Rev. D* **111**, 026010 (2025).
 [23] Joel Scherk and John H Schwarz, “Dual models and the geometry of space-time,” *Physics Letters B* **52**, 347–350 (1974).
 [24] Michael K Murray, “Bundle gerbes,” *Journal of the London Mathematical Society* **54**, 403–416 (1996).
 [25] Alan L Carey, Jouko Mickelsson, and Michael K Murray, “Bundle gerbes applied to quantum field theory,” *Reviews in Mathematical Physics* **12**, 65–90 (2000).
 [26] Giandomenico Palumbo and Nathan Goldman, “Revealing tensor monopoles through quantum-metric measurements,” *Phys. Rev. Lett.* **121**, 170401 (2018).
 [27] Giandomenico Palumbo and Nathan Goldman, “Tensor Berry connections and their topological invariants,” *Phys. Rev. B* **99**, 045154 (2019).
 [28] Yan-Qing Zhu, Nathan Goldman, and Giandomenico Palumbo, “Four-dimensional semimetals with tensor monopoles: From surface states to topological responses,” *Phys. Rev. B* **102**, 081109 (2020).

- [29] Yan-Qing Zhu, Wen Zheng, Shi-Liang Zhu, and Giandomenico Palumbo, “Band topology of pseudo-Hermitian phases through tensor Berry connections and quantum metric,” *Phys. Rev. B* **104**, 205103 (2021).
- [30] Giandomenico Palumbo, “Non-Abelian tensor Berry connections in multiband topological systems,” *Phys. Rev. Lett.* **126**, 246801 (2021).
- [31] Shuhei Ohyama and Shinsei Ryu, “Higher structures in matrix product states,” *Phys. Rev. B* **109**, 115152 (2024).
- [32] Ken Shiozaki, Niclas Heinsdorf, and Shuhei Ohyama, “Higher Berry curvature from matrix product states,” (2023), [arXiv:2305.08109 \[quant-ph\]](#).
- [33] Shuhei Ohyama and Shinsei Ryu, “Higher Berry phase from projected entangled pair states in (2+1) dimensions,” (2024), [arXiv:2405.05325 \[cond-mat.str-el\]](#).
- [34] Shuhei Ohyama and Shinsei Ryu, “Higher Berry connection for matrix product states,” *Phys. Rev. B* **111**, 035121 (2025).
- [35] Ophelia Evelyn Sommer, Xueda Wen, and Ashvin Vishwanath, “Higher Berry curvature from the wave function. i. schmidt decomposition and matrix product states,” *Phys. Rev. Lett.* **134**, 146601 (2025).
- [36] Marvin Qi, David T. Stephen, Xueda Wen, Daniel Spiegel, Markus J. Pflaum, Agnès Beaudry, and Michael Hermele, “Charting the space of ground states with tensor networks,” (2025), [arXiv:2305.07700 \[cond-mat.str-el\]](#).
- [37] Stuart Johnson, “Constructions with bundle gerbes,” (2003), [arXiv:math/0312175 \[math.DG\]](#).
- [38] Richard J Szabo, “Quantization of higher abelian gauge theory in generalized differential cohomology,” *arXiv preprint arXiv:1209.2530* (2012).
- [39] Aleksandra Nelson, Titus Neupert, A. Alexandradinata, and Tomáš Bzdušek, “Delicate topology protected by rotation symmetry: Crystalline Hopf insulators and beyond,” *Phys. Rev. B* **106**, 075124 (2022).
- [40] Joel E. Moore, Ying Ran, and Xiao-Gang Wen, “Topological surface states in three-dimensional magnetic insulators,” *Phys. Rev. Lett.* **101**, 186805 (2008).
- [41] Ricardo Kennedy, “Topological Hopf-Chern insulators and the Hopf superconductor,” *Phys. Rev. B* **94**, 035137 (2016).
- [42] Thomas Schuster, Snir Gazit, Joel E. Moore, and Norman Y. Yao, “Floquet Hopf insulators,” *Phys. Rev. Lett.* **123**, 266803 (2019).
- [43] F. Nur Ünal, André Eckardt, and Robert-Jan Slager, “Hopf characterization of two-dimensional Floquet topological insulators,” *Phys. Rev. Res.* **1**, 022003 (2019).
- [44] Hyeonmuk Lim, Sunje Kim, and Bohm-Jung Yang, “Real Hopf insulator,” *Phys. Rev. B* **108**, 125101 (2023).
- [45] Wojciech J. Jankowski, Arthur S. Morris, Zory Davoyan, Adrien Bouhon, F. Nur Ünal, and Robert-Jan Slager, “Non-Abelian Hopf-Euler insulators,” *Phys. Rev. B* **110**, 075135 (2024).
- [46] F. Nur Ünal, Adrien Bouhon, and Robert-Jan Slager, “Topological Euler class as a dynamical observable in optical lattices,” *Phys. Rev. Lett.* **125**, 053601 (2020).
- [47] Alexei Kitaev, “Periodic table for topological insulators and superconductors,” in *AIP Conference Proceedings* (AIP, 2009).
- [48] Daniel S. Freed and Gregory W. Moore, “Twisted equivariant matter,” *Annales Henri Poincaré* **14**, 1927–2023 (2013).
- [49] Jorrit Kruthoff, Jan de Boer, Jasper van Wezel, Charles L. Kane, and Robert-Jan Slager, “Topological classification of crystalline insulators through band structure combinatorics,” *Phys. Rev. X* **7**, 041069 (2017).
- [50] Adrien Bouhon, Tomáš Bzdušek, and Robert-Jan Slager, “Geometric approach to fragile topology beyond symmetry indicators,” *Phys. Rev. B* **102**, 115135 (2020).
- [51] Qian Niu, D. J. Thouless, and Yong-Shi Wu, “Quantized Hall conductance as a topological invariant,” *Phys. Rev. B* **31**, 3372–3377 (1985).
- [52] H. Weisbrich, M. Bestler, and W. Belzig, “Tensor Monopoles in superconducting systems,” *Quantum* **5**, 601 (2021).
- [53] Y. X. Zhao and Y. Lu, “ PT -symmetric real Dirac fermions and semimetals,” *Phys. Rev. Lett.* **118**, 056401 (2017).
- [54] Matthew Reece, “Extra-dimensional axion expectations,” (2025), [arXiv:2406.08543 \[hep-ph\]](#).
- [55] Giandomenico Palumbo, “Boundary Witten effect in multi-axion insulators,” (2025), [arXiv:2504.16919 \[cond-mat.mes-hall\]](#).
- [56] Xiao-Liang Qi, Taylor L. Hughes, and Shou-Cheng Zhang, “Topological field theory of time-reversal invariant insulators,” *Physical Review B* **78** (2008), 10.1103/physrevb.78.195424.
- [57] Andrei Malashevich and Ivo Souza, “Band theory of spatial dispersion in magnetoelectrics,” *Phys. Rev. B* **82**, 245118 (2010).
- [58] Andrei Malashevich, Ivo Souza, Sinisa Coh, and David Vanderbilt, “Theory of orbital magnetoelectric response,” *New Journal of Physics* **12**, 053032 (2010).
- [59] Xiao-Liang Qi and Shou-Cheng Zhang, “Topological insulators and superconductors,” *Rev. Mod. Phys.* **83**, 1057–1110 (2011).
- [60] Ken Shiozaki and Satoshi Fujimoto, “Electromagnetic and thermal responses of Z topological insulators and superconductors in odd spatial dimensions,” *Physical Review Letters* **110** (2013).
- [61] Junyeong Ahn, Su-Yang Xu, and Ashvin Vishwanath, “Theory of optical axion electrodynamics and application to the Kerr effect in topological antiferromagnets,” *Nature Communications* **13**, 7615 (2022).
- [62] A. Alexandradinata, Aleksandra Nelson, and Alexey A. Soluyanov, “Teleportation of Berry curvature on the surface of a Hopf insulator,” *Phys. Rev. B* **103**, 045107 (2021).
- [63] S.-T. Wang, D.-L. Deng, Joel E. Moore, Kai Sun, and L.-M. Duan, “Quantized electromagnetic response of three-dimensional chiral topological insulators,” *Phys. Rev. B* **91**, 035108 (2015).
- [64] See Supplemental Material (SM) at [url] for details on the homotopy classification and models of different Hopf insulators (Sec. I), and the underlying tensor monopoles and gerbe structures (Sec. II). The Supplemental Material also contains Refs. [81–83].
- [65] Junyeong Ahn, Sungjoon Park, and Bohm-Jung Yang, “Failure of Nielsen-Ninomiya theorem and fragile topology in two-dimensional systems with space-time inversion symmetry: Application to twisted bilayer graphene at magic angle,” *Phys. Rev. X* **9**, 021013 (2019).
- [66] Adrien Bouhon, QuanSheng Wu, Robert-Jan Slager, Hongming Weng, Oleg V. Yazyev, and Tomáš Bzdušek, “Non-Abelian reciprocal braiding of Weyl points and its manifestation in ZrTe,” *Nature Physics* **16**, 1137–1143 (2020).
- [67] Adrien Bouhon, Abigail Timmel, and Robert-Jan Slager, “Quantum geometry beyond projective single bands,” (2023), [arXiv:2303.02180 \[cond-mat.mes-hall\]](#).
- [68] Bastien Lapierre, Titus Neupert, and Luka Trifunovic, “ N -band Hopf insulator,” *Phys. Rev. Res.* **3**, 033045 (2021).
- [69] Junyeong Ahn, Guang-Yu Guo, and Naoto Nagaosa, “Low-frequency divergence and quantum geometry of the bulk photovoltaic effect in topological semimetals,” *Phys. Rev. X* **10**, 041041 (2020).
- [70] Junyeong Ahn, Guang-Yu Guo, Naoto Nagaosa, and Ashvin Vishwanath, “Riemannian geometry of resonant optical responses,” *Nature Physics* **18**, 290–295 (2021).
- [71] Wojciech J. Jankowski and Robert-Jan Slager, “Quantized inte-

grated shift effect in multigap topological phases,” *Phys. Rev. Lett.* **133**, 186601 (2024).

- [72] V. I. Belinicher, E. L. Ivchenko, and B. I. Sturman, “Kinetic theory of the displacement photovoltaic effect in piezoelectric,” *Soviet Journal of Experimental and Theoretical Physics* **56**, 359 (1982).
- [73] J. E. Sipe and Ed Ghahramani, “Nonlinear optical response of semiconductors in the independent-particle approximation,” *Phys. Rev. B* **48**, 11705–11722 (1993).
- [74] Takahiro Morimoto and Naoto Nagaosa, “Topological nature of nonlinear optical effects in solids,” *Science Advances* **2**, e1501524 (2016).
- [75] Ashley M. Cook, Benjamin M. Fregoso, Fernando de Juan, Sinisa Coh, and Joel E. Moore, “Design principles for shift current photovoltaics,” *Nature Communications* **8** (2017).
- [76] A. Alexandradinata, “Quantization of intraband and interband Berry phases in the shift current,” *Phys. Rev. B* **110**, 075159 (2024).
- [77] Zory Davoyan, Wojciech J. Jankowski, Adrien Bouhon, and Robert-Jan Slager, “Three-dimensional \mathcal{PT} -symmetric topological phases with a Pontryagin index,” *Phys. Rev. B* **109**, 165125 (2024).
- [78] C. Repellin and N. Goldman, “Detecting fractional Chern insulators through circular dichroism,” *Phys. Rev. Lett.* **122**, 166801 (2019).
- [79] Matthew B. Hastings and Spyridon Michalakis, “Quantization of Hall conductance for interacting electrons on a torus,” *Communications in Mathematical Physics* **334**, 433–471 (2015).
- [80] Sven Bachmann, Alex Bols, Wojciech De Roeck, and Martin Fraas, “Quantization of conductance in gapped interacting systems,” *Annales Henri Poincaré* **19**, 695–708 (2018).
- [81] Thorsten B. Wahl, Wojciech J. Jankowski, Adrien Bouhon, Gaurav Chaudhary, and Robert-Jan Slager, “Exact projected entangled pair ground states with topological Euler invariant,” *Nature Communications* **16** (2025).
- [82] Wojciech J. Jankowski, Arthur S. Morris, Adrien Bouhon, F. Nur Ünal, and Robert-Jan Slager, “Optical manifestations and bounds of topological Euler class,” *Phys. Rev. B* **111**, L081103 (2025).
- [83] Ashwat Jain, Wojciech J. Jankowski, and Robert-Jan Slager, “Anomalous geometric transport signatures of topological Euler class,” *Phys. Rev. B* **111**, 235149 (2025).

END MATTER

Appendix A: More details on gerbes.— The gerbe connection can be constructed from the contact structure constituted by a triplet of scalar fields $(\phi_1^\chi, \phi_2^\chi, \phi_3^\chi)$ over a base space, which in the context of this work is the k -space [27]. We set the flavours χ to run over the orbital basis $\chi = A, B, \dots$. The ϕ_a^χ fields, which encode the contact structure, define a tensor connection [27],

$$B_{ij}^{nm} = \frac{i}{3} \varepsilon_{abc} \sum_{\chi} \phi_a^\chi \partial_i \phi_b^\chi \partial_j \phi_c^\chi, \quad (16)$$

with $a, b, c = 1, 2, 3$. We choose $\phi_1^\chi = u_n^\chi$, $\phi_2^\chi = (u_m^\chi)^*$, $\phi_3^\chi = \phi_{nm}$, with $u_n^\chi \equiv [|u_{n\mathbf{k}}\rangle]_\chi$ the Bloch orbital coefficients, and ϕ_{nm} the Wilson line pseudoscalar, obtaining the tensor connection defined in the main text. Notably, for B_{ij}^{nn} ($n = m$), under a gauge transformation $u_n^\chi \rightarrow e^{i\alpha_n} u_n^\chi$, we have: $\phi_1^\chi \rightarrow e^{i\alpha_n} \phi_1^\chi$, $\phi_2^\chi \rightarrow e^{-i\alpha_n} \phi_2^\chi$, $\phi_3^\chi \rightarrow \phi_3^\chi + \alpha_n$, consistently with the gerbe connection definitions of Ref. [27], and consistently with the transformation, $\phi_{nn}(\mathbf{k}) \rightarrow \phi_{nn}(\mathbf{k}) + \alpha_n(\mathbf{k})$, as demonstrated in the main text.

Appendix B: Further details on Kalb-Ramond flux in quantized topological ME response.— We here include more technical detail on how the gerbe connection arises in the magnetoelectric (ME) response. The magnetoelectric tensor providing for magnetization response $M_i = \alpha_{ij} E_j$ to electric field E_j can be decomposed in terms of two terms $\alpha_{ij} = \alpha_{ij}^{\text{top}} + \alpha_{ij}^{\text{non-top}}$, following Ref. [57], with a topological contribution central to this work,

$$\alpha_{ij}^{\text{top}} = \frac{e^2}{2\hbar c} \int_{\text{BZ}} \frac{d^3\mathbf{k}}{(2\pi)^3} \sum_{n,n'}^{\text{occ}} \text{Re} \varepsilon_{jkl} \langle u_{n\mathbf{k}} | \partial_i u_{n'\mathbf{k}} \rangle \langle \partial_k u_{n'\mathbf{k}} | \partial_l u_{n\mathbf{k}} \rangle. \quad (17)$$

In the above, n, n' run over the occupied bands (occ). We stress that the topological part provides for a \mathbb{Z} -quantized contribution to a magnetoelectric response. In particular, α_{ij}^{top} can be larger than the Chern-Simons contribution $\theta = \pi$, equal in magnitude to a contribution arising from $\mathcal{DD} = 1$. In the real material context, the topological contributions are known to dominate the other, i.e., nontopological contributions [58], to magnetoelectric coupling. On rewriting α_{ij}^{top} in terms of Berry connections,

$$\alpha_{ij}^{\text{top}} = \frac{e^2}{2\hbar c} \int_{\text{BZ}} \frac{d^3\mathbf{k}}{(2\pi)^3} \sum_{n,n'}^{\text{occ}} \text{Re} \varepsilon_{jkl} A_i^{nn'} \partial_k A_l^{n'n}. \quad (18)$$

and on combining with the definition $B_{ij}^{nn'}$ from the main text,

$$\begin{aligned} \text{Tr} \alpha_{ij}^{\text{top}} &= \frac{e^2}{2\hbar c} \int_{\text{BZ}} \frac{d^3\mathbf{k}}{(2\pi)^3} \sum_{n,n'}^{\text{occ}} (\partial_x B_{yz}^{nn'} + \partial_y B_{zx}^{nn'} + \partial_z B_{xy}^{nn'}) \\ &= \frac{e^2}{2\hbar c} \int_{\text{BZ}} \frac{d^3\mathbf{k}}{(2\pi)^3} \sum_{n,n'}^{\text{occ}} \mathcal{H}_{xyz}^{nn'}, \end{aligned} \quad (19)$$

which demonstrates the presence of the Kalb-Ramond flux $\mathcal{H}_{xyz}^{nn'}$, i.e., higher tensor Berry curvature, in the magnetoelectric response. Importantly, $\text{Tr } \alpha_{ij}^{\text{top}}$ is in general *not* just a Chern-Simons angle θ_{CS} , consistently with the observations of Ref. [61]. On the other hand, the nontopological contribution $\alpha_{ij}^{\text{non-top}}$ reads [57],

$$\alpha_{ij}^{\text{non-top}} = \frac{e^2}{\hbar c} \int_{\text{BZ}} \frac{d^3 \mathbf{k}}{(2\pi)^3} \sum_n^{\text{occ}} \sum_m^{\text{unocc}} \text{Re} \left(\varepsilon_{jkl} \frac{\langle \partial_k u_{n\mathbf{k}} | \partial_l (H + E_{n\mathbf{k}}) | u_{m\mathbf{k}} \rangle \langle u_{m\mathbf{k}} | \partial_i u_{n\mathbf{k}} \rangle}{E_{m\mathbf{k}} - E_{n\mathbf{k}}} \right), \quad (20)$$

with m running over the unoccupied bands (unocc), for a Hamiltonian H and band energies $E_{n\mathbf{k}}$. We also evaluate $\alpha_{ij}^{\text{non-top}}$ in the main text for comparison. We find the contribution $\alpha_{ij}^{\text{non-top}}$ to be dominated by the topological contribution α_{ij}^{top} (see Fig. 3), consistently with the findings of Ref. [58] concerning general magnetoelectric media constituted by the known materials.

Appendix C: Details on torsion and quantized shift response.— We here provide further technical details showing how the gerbe structure arises from the torsion in the quantized integrated shift effect [71] in response to the circularly polarized light. The circular shift photoconductivity $\sigma_{ijk}^{\text{shift,C}}(\omega) = \text{Im } \sigma_{ijk}^{\text{shift}}(\omega)$ [69] amounts to,

$$\sigma_{ijk}^{\text{shift,C}}(\omega) = \frac{\pi e^3}{\hbar^2} \int_{\text{BZ}} \frac{d^3 \mathbf{k}}{(2\pi)^3} \text{Re} \sum_{n,m} f_{nm} \left(C_{kij}^{nm} - (C_{jik}^{nm})^* \right) \times \delta(\omega - \omega_{mn}), \quad (21)$$

where $\omega_{mn} \equiv (E_{m\mathbf{k}} - E_{n\mathbf{k}})/\hbar$ is an energy difference, and f_{nm} are the occupation factor differences. The Hermitian connection reads $C_{ijk}^{nm} \equiv A_i^{nm} \mathcal{D}_j^{nm} A_k^{mn}$, with a covariant derivative, $\mathcal{D}_i^{nm} \equiv \partial_i - i(A_i^{nn} - A_i^{mm})$ [70]. The interband torsion is defined as $\mathcal{T}_{ijk}^{nm} \equiv C_{ijk}^{nm} - C_{ikj}^{nm}$, and is antisymmetric in the pair of indices $\mathcal{T}_{ijk}^{nm} = -\mathcal{T}_{ikj}^{nm}$ by construction. A spectral integration over frequencies ω and an antisymmetrization over all three spatial indices obtain the left-hand side of Eq. (11) in terms of torsion, which yields the shift current sum rule originally identified in Ref. [71]. Correspondingly, on substituting Hermitian connection and comparing with the tensor connection B_{ij}^{nm} definition from the main text; in the presence of a trivialized connection term in the covariant derivative $\mathcal{D}_i^{nm} \rightarrow \partial_i$ taken in the parallel transport gauge, we have,

$$\mathcal{T}_{ijk}^{nm} + \mathcal{T}_{jki}^{nm} + \mathcal{T}_{kij}^{nm} = \partial_i B_{jk}^{nm} + \partial_j B_{ki}^{nm} + \partial_k B_{ij}^{nm} \equiv \mathcal{H}_{ijk}^{nm}. \quad (22)$$

Hence, we demonstrated that the interband torsion \mathcal{T}_{ijk}^{nm} amounts to the Kalb-Ramond flux \mathcal{H}_{ijk}^{nm} in the momentum space. More precisely, the higher-tensor flux \mathcal{H}_{ijk}^{nm} is the totally antisymmetric part of the torsion \mathcal{T}_{ijk}^{nm} , i.e., $\mathcal{H}_{ijk}^{nm} \propto \mathcal{T}_{[ijk]}^{nm}$, with [...] denoting an antisymmetrization in all three indices. Setting $n = m$ reduces the multiband torsion \mathcal{T}_{ijk}^{nm} to an intraband torsion \mathcal{T}_{ijk}^{nn} , which is not present in the nonlinear shift response, but instead enters the magnetoelectric response through a flux \mathcal{H}_{ijk}^{nn} central to the previous section.

SUPPLEMENTAL MATERIAL

Probing Tensor Monopoles and Gerbe Invariants in Three-Dimensional Topological Matter

Wojciech J. Jankowski,^{1,*} Robert-Jan Slager,^{2,1} and Giandomenico Palumbo^{3,†}

¹*TCM Group, Cavendish Laboratory, University of Cambridge, J. J. Thomson Avenue, Cambridge CB3 0HE, UK*

²*Department of Physics and Astronomy, University of Manchester, Oxford Road, Manchester M13 9PL, UK*

³*School of Theoretical Physics, Dublin Institute for Advanced Studies, 10 Burlington Road, Dublin 4 D04 C932, Ireland*

(Dated: July 31, 2025)

CONTENTS

I. Homotopy classification and models of topological insulators beyond the tenfold way	2
A. Two-band Hopf insulators	2
B. N-band Hopf insulators	3
C. Three-band real Hopf insulators	3
D. Four-band real Hopf insulators	3
E. Three-band real flag phases	4
F. Four-band real flag phases	4
II. Tensor monopoles and gerbe invariants in homotopy-classified topological insulators	4
A. Two-band Hopf insulators	4
B. N-band Hopf insulators	4
C. Three-band real Hopf insulators	5
D. Four-band real Hopf insulators	5
E. Three-band real flag phases	5
F. Four-band real flag phases	5
References	6

* wjj25@cam.ac.uk

† giandomenico.palumbo@gmail.com

I. HOMOTOPY CLASSIFICATION AND MODELS OF TOPOLOGICAL INSULATORS BEYOND THE TENFOLD WAY

In the following, we provide further details on the homotopy classification of unconventional three-dimensional topological insulators falling beyond the notion of stable equivalence underlying K-theory [1].

We begin by introducing the classifying spaces \mathcal{G} , which capture the minimal topology of Hamiltonians $H(\mathbf{k})$ classified as maps from d -dimensional Brillouin zone (BZ) isomorphic to a d -dimensional torus, $\text{BZ} \cong T^d$, where $\mathbf{k} \in \text{BZ}$. The strong topological invariants are imposed within the mapping sequence: $\text{BZ} \cong T^d \rightarrow S^d \rightarrow \mathcal{G}$, classified with homotopy groups $\pi_d[\mathcal{G}]$. The weak invariants can be included on considering more general mappings, $\text{BZ} \cong T^d \rightarrow \mathcal{G}$ classified by homotopy classes $[T^d, \mathcal{G}]$. Centrally to this work, in the following, we focus on $d = 3$.

In the absence of additional symmetries other than $U(1)$ for particle/charge conservation, the corresponding classifying spaces for the Hamiltonians are complex flag manifolds,

$$\text{Fl}_{p_1, \dots, p_k}(\mathbb{C}) \cong \frac{U(N)}{U(p_1) \times \dots \times U(p_k)}, \quad (1)$$

for $i = 1, 2, \dots, k$, where i labels each of the k band subspaces (subbundles) of rank p_k equal to the number of bands therein. Each isolated subspace admits a gauge group $G_{p_i} = U(p_i)$ [2] associated with the gauge transformations in the degenerate subspace. Importantly, the presence of a spinless $(PT)^2 = +1$ symmetry in the Hamiltonians results in an existence of a real gauge and a modified classification by real flag manifolds, $\text{Fl}_{p_1, \dots, p_k}(\mathbb{R}) \cong \frac{O(N)}{O(p_1) \times \dots \times O(p_k)}$, on replacing each unitary gauge group with an orthogonal one: $U(p_k) \rightarrow O(p_k)$. Moreover, the classification can be further refined by defining the so-called orientable phases classified by oriented flag manifolds $\text{Fl}_{p_1, \dots, p_k}^+(\mathbb{C})$, $\text{Fl}_{p_1, \dots, p_k}^+(\mathbb{R})$, where the orientability condition is imposed on replacements $U(p_k) \rightarrow \text{SU}(p_k)$, $O(p_k) \rightarrow \text{SO}(p_k)$ in the corresponding definitions [2].

A. Two-band Hopf insulators

We begin with two-band Hopf insulators [3, 4]. The classifying space of a two-band Hopf insulator is a complex Grassmannian $\text{Gr}_{1,2}(\mathbb{C}) \equiv \text{Fl}_{1,1}(\mathbb{C})$:

$$\text{Gr}_{1,2}(\mathbb{C}) \cong \frac{U(2)}{U(1) \times U(1)} \cong \frac{\text{SU}(2)}{U(1)} \cong S^2, \quad (2)$$

with the third homotopy group classifying three-dimensional bulk phases [3],

$$\pi_3[\text{Gr}_{1,2}(\mathbb{C})] \cong \pi_3[S^2] \cong \mathbb{Z}. \quad (3)$$

$\pi_3[S^2] \cong \mathbb{Z}$ classifies distinct Hopf fibrations: $S^3 \rightarrow S^2$. In the above, we assumed an absence of weak invariants. In the presence of weak invariants, the nontrivial subdimensional Chern numbers $(C_x, C_y, C_z) = \mathbb{Z}^3$, one realizes Hopf-Chern insulator [4] classified by homotopy classes of maps $T^3 \rightarrow \text{Gr}_{1,2}(\mathbb{C}) \cong S^2$,

$$[T^3, S^2] = \left\{ (\chi; \mathbf{C}) \mid \mathbf{C} = (C_x, C_y, C_z) \in \mathbb{Z}^3; \right. \\ \left. \chi \in \begin{cases} \mathbb{Z} & \mathbf{C} = 0 \\ \mathbb{Z}_{2 \text{gcd}(\mathbf{C})} & \mathbf{C} \neq 0 \end{cases} \right\}, \quad (4)$$

where $\text{gcd}(\mathbf{C})$ is the greatest common divisor of the integer weak Chern numbers. The index χ corresponds to the strong Hopf invariant. If the Chern numbers are trivial $(C_x, C_y, C_z) = (0, 0, 0) = 0$, the homotopy classes reduce to the original Hopf invariant.

To retrieve the tensor monopole in the two-band Hopf insulators in the main text, we adapt the models of Refs. [3, 4]. The studied two-band Hamiltonian $H(\mathbf{k}) = \mathbf{d}(\mathbf{k}) \cdot \boldsymbol{\sigma}$ decomposed in the basis of Pauli matrices $\boldsymbol{\sigma} = (\sigma_x, \sigma_y, \sigma_z)$ is generated by a vector,

$$\mathbf{d}(\mathbf{k}) = \begin{pmatrix} \cos k_z \sin k_x - \sin k_z \sin k_y \\ \sin k_z \sin k_x + \cos k_z \sin k_y \\ M - \cos k_x - \cos k_y \end{pmatrix}, \quad (5)$$

where M is a topological mass parameter yielding nontrivial Hopf invariant $\chi = \mathcal{D}\mathcal{D}_{11} = 1$, when $|M| < 2$.

B. N -band Hopf insulators

The generalization of a two-band Hopf insulator to a N -band Hopf insulator was introduced in Ref. [5]. The N -band insulator realizes $N \geq 2$ isolated single bands constituting Bloch subbundles \mathcal{B}_i , each with gauge group $G_i = \text{U}(1)$. In the isolated band limit, the classifying space reduces to,

$$\text{Fl}_{1,\dots,1}(\mathbb{C}) \cong \frac{\text{U}(N)}{\text{U}(1)^N}, \quad (6)$$

which realizes a nontrivial third homotopy group [5],

$$\pi_3[\text{Fl}_{1,\dots,1}(\mathbb{C})] \cong \pi_3[\text{SU}(N)] \cong \pi_3[S^2] \cong \mathbb{Z}, \quad (7)$$

classifying distinct Hopf fibrations analogously to the two-band Hopf insulator.

C. Three-band real Hopf insulators

On imposing a reality condition with \mathcal{PT} symmetry [2], we now focus on three-band real Hopf insulators with a topologically non-trivial two-band subspace ($p_1 = 2$), and a trivial third band $p_2 = 1$ [6]. The classifying space of a three-band real Hopf insulator is a real Grassmannian $\text{Gr}_{2,3}(\mathbb{R}) \equiv \text{Fl}_{2,1}(\mathbb{R})$,

$$\text{Gr}_{2,3}(\mathbb{R}) \cong \frac{\text{O}(3)}{\text{O}(2) \times \text{O}(1)} \cong \mathbb{RP}^2, \quad (8)$$

$$\pi_3[\text{Gr}_{2,3}(\mathbb{R})] \cong \pi_3[\mathbb{RP}^2] \cong \pi_3[S^2] \cong \mathbb{Z}, \quad (9)$$

which defines the strong Hopf index $\mathcal{H} \in \mathbb{Z}$. The presence of weak subdimensional Euler invariants [2, 6–14] in two-dimensional BZ subtori allows for nontrivial indices $(\chi_x, \chi_y, \chi_z) \in \mathbb{Z}^3$, which when nontrivial, realize the so-called Hopf-Euler topology [6]. The (orientable) Hopf-Euler insulators are respectively classified by homotopy classes of maps $T^3 \rightarrow \text{Gr}_{2,3}^+(\mathbb{R}) \cong S^2$ [6],

$$[T^3, S^2] = \left\{ (\mathcal{H}; \boldsymbol{\chi}) \left| \begin{array}{l} \boldsymbol{\chi} = (\chi_x, \chi_y, \chi_z) \in \mathbb{Z}^3; \\ \mathcal{H} \in \left\{ \begin{array}{ll} \mathbb{Z} & \boldsymbol{\chi} = 0 \\ \mathbb{Z}_{\text{gcd}(\boldsymbol{\chi})} & \boldsymbol{\chi} \neq 0 \end{array} \right\} \end{array} \right. \right\}, \quad (10)$$

where $\text{gcd}(\boldsymbol{\chi})$ is the greatest common divisor of the integer weak Euler invariants. The index \mathcal{H} corresponds to the strong Hopf invariant. When the weak Euler numbers are trivial $(\chi_x, \chi_y, \chi_z) = (0, 0, 0) = 0$, the homotopy classes reduce to the original real Hopf invariant.

The interband momentum-space tensor Berry connections and magnetoelectric response studied in the main text were retrieved from the model introduced in Ref. [6]. The corresponding three-band Hamiltonian reads: $H(\mathbf{k}) = 2\mathbf{d}(\mathbf{k}) \otimes \mathbf{d}^T(\mathbf{k}) - \text{diag}(1, 1, 1)$ with $\mathbf{d}(\mathbf{k})$ defined in Eq. (5), and where a small diagonal perturbation was added to split the degeneracy of the occupied two-band subspace. The higher Hopf index can be generated by sending $k_z \rightarrow pk_z$, with $p \in \mathbb{N}$. The topological phase with $\mathcal{DD}_{12} = \mathcal{H} = p$ is retrieved on setting $|M| \leq 2$.

D. Four-band real Hopf insulators

Further to the three-band real Hopf insulator, we now focus on the four-band real Hopf insulators with two isolated two-band subspace ($p_1 = 2$), and ($p_2 = 1$) [11]. The classifying space of a three-band real Hopf insulator is a real Grassmannian $\text{Gr}_{2,4}(\mathbb{R}) \equiv \text{Fl}_{2,2}(\mathbb{R})$,

$$\text{Gr}_{2,4}(\mathbb{R}) \cong \frac{\text{O}(4)}{\text{O}(2) \times \text{O}(2)}, \quad (11)$$

$$\pi_3[\text{Gr}_{2,4}(\mathbb{R})] \cong \pi_3[S^2] \oplus \pi_3[S^2] \cong \mathbb{Z} \times \mathbb{Z}, \quad (12)$$

which defines a pair of integer real Hopf indices $(\mathcal{H}_1, \mathcal{H}_2) \in \mathbb{Z}^2$.

E. Three-band real flag phases

Under the partitioning of three isolated real bands, the classifying space becomes a real flag manifold distinct from the Grassmannians outlined above, defining the so-called real flag phases [6, 15] classified by,

$$\text{Fl}_{1,1,1}(\mathbb{R}) \cong \frac{\text{O}(3)}{\text{O}(1) \times \text{O}(1) \times \text{O}(1)}, \quad (13)$$

which realizes nontrivial homotopy elements,

$$\pi_3[\text{Fl}_{1,1,1}(\mathbb{R})] \cong \pi_3[S^3] \cong \mathbb{Z}. \quad (14)$$

The single flag index $w \in \mathbb{Z}$ can be viewed as a single three-dimensional Pontryagin index [6, 15].

F. Four-band real flag phases

Analogously to the three-band case, the presence of four real bands with multiple gaps [6, 15], realizes more general flag limits, beyond the previously mentioned Grassmannians. In the isolated limit of four real bands, the classifying space reads,

$$\text{Fl}_{1,1,1,1}(\mathbb{R}) \cong \frac{\text{O}(4)}{\text{O}(1) \times \text{O}(1) \times \text{O}(1) \times \text{O}(1)}, \quad (15)$$

which results in nontrivial homotopy group elements [15],

$$\pi_3[\text{Fl}_{1,1,1,1}(\mathbb{R})] \cong \pi_3\left[\frac{S^3 \times S^3}{\mathbb{Z}^2}\right] \cong \pi_3[S^3] \oplus \pi_3[S^3] \cong \mathbb{Z} \times \mathbb{Z}. \quad (16)$$

The nontrivial homotopy elements define a pair of flag indices $(w_L, w_R) \in \mathbb{Z}^2$ which can be viewed as isoclinic winding numbers $\pi_3[S^3] \cong \mathbb{Z}$ acting on the individual hyperspheres S^3 [6, 15].

II. TENSOR MONOPOLES AND GERBE INVARIANTS IN HOMOTOPY-CLASSIFIED TOPOLOGICAL INSULATORS

In the following, we detail the constructions of tensor Berry connection monopoles, i.e., topologically nontrivial configurations of momentum-space Kalb-Ramond fields B_{ij} in the homotopy-classified topological insulators introduced in the previous section. Hence, we respectively map the relevant Hopf and Pontryagin indices to the \mathcal{DD} invariants of nontrivial gerbe bundles constructed out of Bloch states.

A. Two-band Hopf insulators

Centrally to this work, we show that a two-band Hopf insulator realizes one momentum-space tensor monopole B_{ij}^{11} with connection 2-form $B^{11} = B_{ij}^{11} dk^i \wedge dk^j$, with Kalb-Ramond flux $\mathcal{H}^{11} = dB^{11}$ determined by its exterior derivative yielding a divergence shown in the main text. Consistently with the construction outlined in the main text, the $\mathcal{DD}_{11} \in \mathbb{Z}$ invariant reads,

$$\mathcal{DD}_{11} = -\frac{1}{4\pi^2} \int_{\text{BZ}} \mathcal{H}^{11} = \chi. \quad (17)$$

B. N-band Hopf insulators

Analogously to a two-band Hopf insulator [3], the N -band Hopf insulator [5] with band n realizing a nontrivial Abelian Chern-Simons 3-form $\mathcal{CS}^n = \varepsilon_{abc} A_a^n \partial_b A_c^n$ [5], hosts a single tensor monopole B_{ij}^{nn} with connection 2-form $B^{nn} = B_{ij}^{nn} dk^i \wedge dk^j$ and Kalb-Ramond flux $\mathcal{H}^{nn} = dB^{nn}$. The supported nontrivial $\mathcal{DD}_{nn} \in \mathbb{Z}$ invariant reads,

$$\mathcal{DD}_{nn} = -\frac{1}{4\pi^2} \int_{\text{BZ}} \mathcal{H}^{nn}, \quad (18)$$

where the explicit form of the tensor Berry connection in band n is obtained by repeating the pseudoscalar $[\phi_{nn}(\mathbf{k})]$ construction outlined in the main text.

C. Three-band real Hopf insulators

We now elaborate on the three-band real Hopf insulators [6], which, as identified in this work, are the condensed matter realizations of an interband tensor monopole in momentum-space Kalb-Ramond fields B_{ij}^{12} defining a connection 2-form $B^{12} = B_{ij}^{12} dk^i \wedge dk^j$. The higher (Berry) curvature realized in the tensor Berry connection B_{ij}^{12} obtains the Kalb-Ramond flux $\mathcal{H}^{12} = dB^{12}$, consistently with the main text. The supported nontrivial interband $\mathcal{DD}_{12} \in \mathbb{Z}$ invariant reads,

$$\mathcal{DD}_{12} = -\frac{1}{4\pi^2} \int_{\text{BZ}} \mathcal{H}^{12} = \mathcal{H}, \quad (19)$$

which amounts to the integer real Hopf index $\mathcal{H} \in \mathbb{Z}$ as a single momentum-space tensor monopole invariant.

D. Four-band real Hopf insulators

We now demonstrate that a four-band real Hopf insulator [11] realizes two tensor monopoles B_{ij}^{12}, B_{ij}^{34} defining connection 2-forms $B^{12} = B_{ij}^{12} dk^i \wedge dk^j$, $B^{34} = B_{ij}^{34} dk^i \wedge dk^j$ and Kalb-Ramond fluxes $\mathcal{H}^{12} = dB^{12}$, $\mathcal{H}^{34} = dB^{34}$ under the choice of a real gauge. These determine a pair of \mathcal{DD} invariants $(\mathcal{DD}_{12}, \mathcal{DD}_{34}) \in \mathbb{Z}^2$,

$$\mathcal{DD}_{12} = -\frac{1}{4\pi^2} \int_{\text{BZ}} \mathcal{H}^{12}, \quad (20)$$

$$\mathcal{DD}_{34} = -\frac{1}{4\pi^2} \int_{\text{BZ}} \mathcal{H}^{34}, \quad (21)$$

which combined amount to the sum of the pair of Hopf invariants, $\mathcal{DD}_{12} + \mathcal{DD}_{34} = \mathcal{H}_1 + \mathcal{H}_2$.

E. Three-band real flag phases

Similarly to the three-band Hopf insulator, the three-band multigap flag phases [6] realize a single tensor monopole in the connection B_{ij}^{12} . Following the construction introduced in the main text, a pair of neighboring bands defines a momentum-space Kalb-Ramond field B_{ij}^{12} and a connection 2-form $B^{12} = B_{ij}^{12} dk^i \wedge dk^j$. The Kalb-Ramond flux reads $\mathcal{H}^{12} = dB^{12}$, and the interband \mathcal{DD} invariant amounts to,

$$\mathcal{DD}_{12} = -\frac{1}{4\pi^2} \int_{\text{BZ}} \mathcal{H}^{12} = w, \quad (22)$$

hence, the flag index $w \in \mathbb{Z}$ is a \mathcal{DD} invariant of the gerbe bundle realized in three isolated bands.

F. Four-band real flag phases

Analogously to the four-band real Hopf insulator, the four-band flag phases [15] realize two tensor monopoles B_{ij}^{12}, B_{ij}^{34} , with connection 2-forms $B^{12} = B_{ij}^{12} dk^i \wedge dk^j$, $B^{34} = B_{ij}^{34} dk^i \wedge dk^j$ and Kalb-Ramond fluxes $\mathcal{H}^{12} = dB^{12}$, $\mathcal{H}^{34} = dB^{34}$ defined in the real gauge. The pair of \mathcal{DD} invariants $(\mathcal{DD}_{12}, \mathcal{DD}_{34}) \in \mathbb{Z}^2$ reads,

$$\mathcal{DD}_{12} = -\frac{1}{4\pi^2} \int_{\text{BZ}} \mathcal{H}^{12}, \quad (23)$$

$$\mathcal{DD}_{34} = -\frac{1}{4\pi^2} \int_{\text{BZ}} \mathcal{H}^{34}, \quad (24)$$

which sums to the pair of isoclinic winding numbers [15] classified in the previous section, i.e., $\mathcal{DD}_{12} + \mathcal{DD}_{34} = w_L + w_R$.

-
- [1] A. Kitaev, in *AIP Conference Proceedings* (AIP, 2009).
 - [2] A. Bouhon, T. Bzdušek, and R.-J. Slager, *Phys. Rev. B* **102**, 115135 (2020).
 - [3] J. E. Moore, Y. Ran, and X.-G. Wen, *Phys. Rev. Lett.* **101**, 186805 (2008).
 - [4] R. Kennedy, *Phys. Rev. B* **94**, 035137 (2016).
 - [5] B. Lapierre, T. Neupert, and L. Trifunovic, *Phys. Rev. Res.* **3**, 033045 (2021).
 - [6] W. J. Jankowski, A. S. Morris, Z. Davoyan, A. Bouhon, F. N. Ünal, and R.-J. Slager, *Phys. Rev. B* **110**, 075135 (2024).
 - [7] J. Ahn, S. Park, and B.-J. Yang, *Phys. Rev. X* **9**, 021013 (2019).
 - [8] A. Bouhon, Q. Wu, R.-J. Slager, H. Weng, O. V. Yazyev, and T. Bzdušek, *Nature Physics* **16**, 1137–1143 (2020).
 - [9] F. N. Ünal, A. Bouhon, and R.-J. Slager, *Phys. Rev. Lett.* **125**, 053601 (2020).
 - [10] A. Bouhon, A. Timmel, and R.-J. Slager, “Quantum geometry beyond projective single bands,” (2023), [arXiv:2303.02180 \[cond-mat.mes-hall\]](#).
 - [11] H. Lim, S. Kim, and B.-J. Yang, *Phys. Rev. B* **108**, 125101 (2023).
 - [12] T. B. Wahl, W. J. Jankowski, A. Bouhon, G. Chaudhary, and R.-J. Slager, *Nature Communications* **16** (2025).
 - [13] W. J. Jankowski, A. S. Morris, A. Bouhon, F. N. Ünal, and R.-J. Slager, *Phys. Rev. B* **111**, L081103 (2025).
 - [14] A. Jain, W. J. Jankowski, and R.-J. Slager, *Phys. Rev. B* **111**, 235149 (2025).
 - [15] Z. Davoyan, W. J. Jankowski, A. Bouhon, and R.-J. Slager, *Phys. Rev. B* **109**, 165125 (2024).